Fundamental study on the effect of grain size distribution on angle of repose

Shintaro Kajiyama[1*], *Yukio* Nakata[2], and *Hitoshi* Nakase[3]

[1]*University of Yamanashi, Graduate Faculty of Interdisciplinary Research, 4-4-37, Takeda, Kofu, Yamanashi, 400-8511 Japan*
[2]*Yamaguchi University, Graduate School of Sciences and Technology for Innovation, 2-16-1 Tokiwadai, Ube, Yamaguchi, 755-8611*
[3]*Tokyo Electric Power Services Co.,Ltd. Research and Business Incubation Unit, 9F,KDX Toyosu Gransquare, 1-7-12 , Shinonome, Koto-ku, Tokyo 135-0062*
[#]Corresponding author: skajiyama@yamanashi.ac.jp

ABSTRACT

In this study, the authors developed a new sidewall velocity-controlled cylindrical angle of repose measurement apparatus that can capture images of a sand heap continuously using two orthogonal cameras in order to reduce the cost of photography. The developed apparatus was used to measure the angle from formation to repose of sand heap using different grain sizes distribution and to assess the effect of grain size distribution on the angle of repose. The formation process of the sand heap was continuously measured using the experimental apparatus, and it was found that the sand heap became steady state when it reached a certain height. It is inferred that the angle of repose measured in a stationary state indicates the inclination angle of the sand heap at a certain point in time, suggesting the possibility of obtaining a highly accurate angle of repose with fewer experiments by using this experimental apparatus to continuously acquire and average the inclination angle of a sand heap in a steady state. For samples with a stepped grain size distribution, the angle of repose was found to be higher than for samples with a gentle grain size distribution at the same 20% grain size D_{20} and mean grain size D_{50}. It was found that the angle of repose increased logarithmically with increasing coefficient of uniformity. Based on these results, it is clear that for a well-graded sand, it is the grain size rather than the coefficient of uniformity that has an effect on the angle of repose.

Keywords: angle of repose; grain size distribution, coefficient of uniformity

1. Introduction

The influence of grain size distribution on the shear properties of sand has been noted in previous studies (e.g. Indraratna et al., 2016, Wang et al., 2013, Viggiani et al., 2001). However, obtaining mechanical properties such as the internal friction angle requires expensive test apparatus such as triaxial testing and long experimental time when experiments are carried out on samples of several grain sizes. Now, measuring the angle of repose is a familiar method for determining the shear properties of the ground. While the angle of repose can be measured easily with simple equipment, it is recognised that there is variability in its value.

For this reason, despite the simplicity of the test, there has been no standardisation of a generic test method. In the United States, ASTM tried to standardize the test method, but it was discontinued because of its limited applicability (ASTM, withdrawn 2005). In Japan, the method for determining the angle of repose, which is specified as an industrial standard by JIS, has a limited application to alumina powders that have passed through a sieve with a 0.2 mm opening (JIS, 1999). This is because the relationship between the electrostatic force and the gravitational force is different depending on the size and density of the particles. For example, the electrostatic force sometimes dominates over the gravitational force. Therefore, the authors decided to investigate the experimental method of the angle of repose for sand.

Because of the lack of established test procedures, there are no standardized methods for making a sand heap, and there are various methods for measuring the resulting sand. There are three main experimental methods: discharge, revolving cylinder and piling. It is noted that even with the same sample, different values of angle of repose can be obtained with these different experimental methods. (Aoki, 1969). Table 1 shows the experimental methods used in previous studies on the angle of repose. The table also includes the results of experiments where the sample was not sand to compare the experimental methods. As can be seen from the table, the shape of the heap can be classified into conical and plane strain conditions, even if they are classified under the same experimental method. For example, in the plane strain type apparatuses such as Botz et al. (2003) and Coetzee and Els (2009), the angle of repose is measured through an observation window on the side. On the other hand, in the case of a cone-shaped apparatus, the apex of the sand heap is not always located at the centre of the cylinder, so that observation from only one direction is insufficient to locate the apex. Miura et al. (1997) erected two scaled posts on the outside of a sand heap and crossed a string

Table 1. List of experimental methods for angle of repose in previous studies

Authors	Method	Details of method	Bottom conditions
Chik and Vallejo (2005)	Piling	Inject materials into the base with a funnel	Flat
Coetzee and Els (2009)	Discharge	Discharge materials from the slit in the centre of the bottom	Flat
Miura et al. (1997)	Discharge, Piling	Inject sand into the base with a funnnel After injecting with afunnnel, lower the side wall to discharge the materials	Flat, Baffle
Chen et al. (2015)	Piling	Inject materials into the base with a funnel	Baffle
Botz et al. (2003)	Revolving cylinder	Rotate the apparatus containing the material	Flat
Wójcik et al. (2018)	Piling	Inject materials on the table	Not mentioned

Authors	Shape of specimen	The size that defines the bottom of the slope	Materials
Chik and Vallejo (2005)	Cone	Free	Sand
Coetzee and Els (2009)	Plane strain	310mm×(Out of plane)730mm 45mm, 80mm (Silo openings)	Corn
Miura et al. (1997)	Cone	Free Φ37.5mm, Φ75.0mm, Φ150.0mm	Glass beads Sand
Chen et al. (2015)	Cone	Φ500mm	Glass beads
Botz et al. (2003)	Plane strain	Unmeasurable (*Φ85×25mm) *Size of the apparatus	Sand
Wójcik et al. (2018)	Cone	Not mentioned	Triticale

between them to directly measure the top of the heap. However, when measuring the granular sand heap physically, it is assumed that a skilful technique is required because the sand flows when the measuring instrument touches the sand heap. Another possible way to directly measure the height of a sand heap is to use a laser displacement meter, but it is not possible to obtain correct results in the case of a highly permeable sample.

Photogrammetry is the realistic method of obtaining accurate angles of repose. Wójcik et al. (2018) carried out computerized photogrammetry by taking a number of photographs from several directions and extracting feature points on the photographs. However, since it is necessary to take images of a single heap in such a way that the feature points appear in several images, many images are required and the cost of taking images is high.

In this study, the authors developed a new sidewall velocity-controlled cylindrical angle of repose measurement apparatus that can capture images of a sand heap continuously using two orthogonal cameras in order to reduce the cost of photography. The developed apparatus was used to measure the angle from formation to repose of sand heap using different grain sizes distribution and to assess the effect of grain size distribution on the angle of repose.

2. Development of testing apparatus and testing method

2.1. Development of experimental equipment

In this study, it was developed a device of the discharge method which is easy to measure or adjust the initial density. The apparatus was designed to allow the side wall of the sand container to descend in anticipation of sand flowing from a stationary state, as typified by slope failure, and a cylindrical shape was adopted to eliminate the influence of the side wall after the sand heap is formed. The external view of the apparatus is shown in Fig. 1 and the schematic diagram is shown in Fig. 2. As shown in Fig. 2, in this experimental apparatus, particles are fed into a space of specimen (a) with a diameter of 160 mm and a height of 100 mm, and then a screw jack (c) is rotated by an electric motor and a speed controller (b) to move the cylindrical wall (d) downwards, thereby controlling the speed at which the particles flow out of the container. The process of sand heap formation is shown in Fig. 3. The lowering of the wall is intended to reduce the amount of sand flowing and to reduce the effect of surface turbulence on the specimen. The top edge of the cylindrical wall (d) is approximately 0.12 mm thick, with a slope of 45° from the edge, not to keep the particles on the wall. A limiter (e) allows the sidewall to be automatically stopped at any height. The bottom of the container (f) and the frame (g) are set horizontally and remain immobile during the

experiment in order to reduce the effect of vibrations on the angle of repose. The discharged particles are collected from the vent (h). The digital cameras x(i) and y(j) are fixed to the bottom of the cylindrical wall in orthogonal positions, and their relative heights to the sidewall are kept constant while the computer (k) takes remote images. The displacement during the experiment is measured by a displacement meter (l), and the displacement is digitally checked by a displacement monitor (m). The displacement speed and the baffle height can be adjusted by the speed controller for each experimental condition.

A fine-tuning valve (n) was also installed in the experimental setup to adjust the position. During the experiment, LED lights (o) are installed in order to clarify the ridges of the sand heap to keep the brightness of the acquired image constant, which facilitates the image analysis. An ionizer is installed above the testing apparatus to remove static electricity from the time the sand is fed into the space.

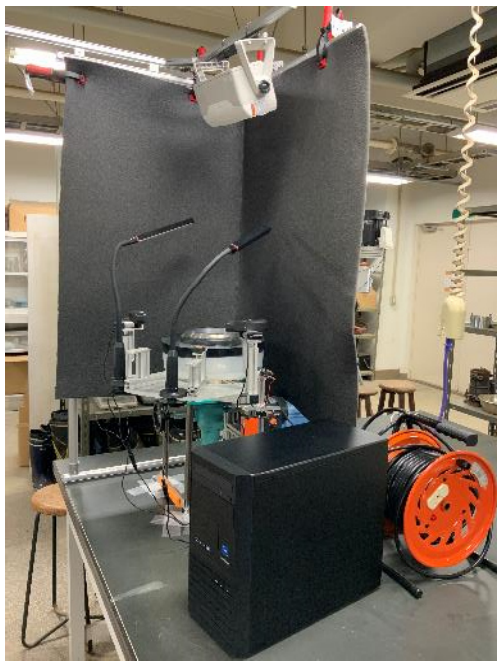

Figure. 1 External view of the experimental apparatus

2.2. Processing for creating verification images

The effect of lens distortion on the image is geometrically corrected using a grid of points with known spacing, as shown in Fig. 4. The first step is to place the geometric correction points on the bottom of the container so that they are perpendicular to the camera lens. The camera is focused and fixed in such a way that the grid of reference points is horizontal and vertical on the screen. This was done for each of the two orthogonal cameras. The 3D coordinates of the vertices were identified from two geometrically corrected images taken from orthogonal positions. The plates of the geometrical correction marks are placed at positions corresponding to the diameter of the cylinder. As shown in Fig. 3, the image taken of the specimen obscures the edge of the cylinder diameter that is orthogonal to the camera. Hence, this image was used to obtain the coordinates of the vertices relative to the centre of the specimen's bottom surface, which is necessary to determine the angle of repose. For one camera x, the coordinates of the vertices of the sand heap were obtained using the following procedure, as shown in Fig.5. First, two edges of the specimen are defined from the image of the geometrical correction points. For these two points, the pixel coordinates origin was set by setting the value of the centre coordinate between the two points in the x-axis direction to 0 and the value of the coordinate in the z-axis direction of the two points to 0. Next, after converting the experimental image to greyscale, edge detection was carried out and the pixel coordinates of the vertices of the sand heap indicated by the green dots in Fig. 5 were calculated in a mechanical way using a computer. The obtained coordinates of the vertices are denoted as (d_x, h_x). Finally, each image was multiplied by the average of the image magnification (mm/pixel) in the x- and z-axis to obtain the coordinates (mm) of each point. At the same time, images were acquired from orthogonal camera y and the coordinates of the vertices (d_y, h_y) were obtained using the same procedure with the vertical direction as the z-axis and the horizontal direction as the y-axis. From these values, the 3D coordinates of the sand heap vertices were determined, using (d_x, d_y) as the coordinates of the horizontal vertex and the average of hx and hy as the height. The average image magnification was 0.168 mm/pix for both cameras.

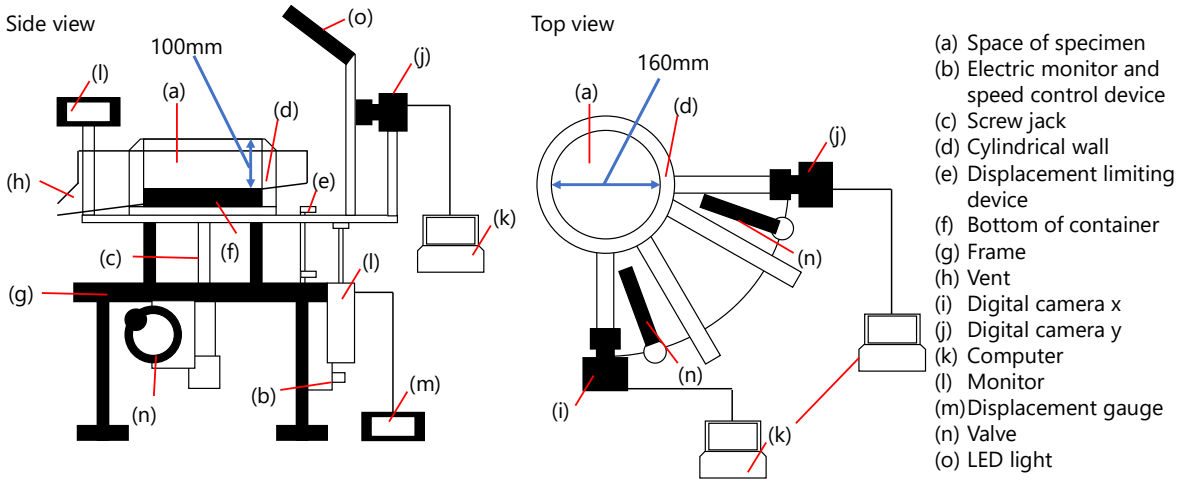

Figure. 2 Schematic of the experimental apparatus

Figure. 3 Formation process of a sand heap

3. Results of AOR measurements using the developed apparatus

3.1. Using materials

The experiments were carried out using five types of samples: three types of silica sand and a mixture of these in arbitrary proportions. The particle size distributions of the samples used in the experiments are shown in Fig.6 and the mixing ratios and particle size properties are shown in Table 2. As shown in Fig.6, Silica C contained 3.8% of particles with a diameter of 0.075 mm or less, while the fine particles in Silica D and E, which were mixed with Silica C, were less than 0.3%. These show that the samples used in this study consisted mostly of sand.

3.2. Test procedure

The sand heap is formed as described in section 2.1 by first placing sand into the space of specimen. After the sand has been placed in the specimen feeding space, the top surface of the specimen is levelled using a straight edge. After adjusting the specimen surface, the ionizer is installed above the testing apparatus. A non-contact static meter is then used to confirm that the static charge on the specimen surface is below 100 V at the start of the experiment. The movable cylindrical wall is then lowered to the desired cylindrical wall height with the ionizer still in operation, and the sand is allowed to flow to form a sand heap. Images were acquired during the sand flow and the angle of repose was measured during the experiment. The lowering speed of the wall was 30 mm/min.

As shown in Table 1, the inclination angles of the sand heap obtained by various methods are all defined as the angle of repose in geotechnical engineering. In geotechnical engineering, it is not specified from which length of the ridge of the sand heap the angle of repose should be determined, so those different observers may measure different angles of repose for the same sand heap. Therefore, in this study, the angle of repose was defined for each of the four measurement methods for the same sand heap.

In the three methods described below, the angle of repose was defined as the angle between the horizontal plane and the line connecting the apex of the sand heap and the top of the cylindrical container, as shown in Fig. 7. The 3D coordinates of this apex were measured from two images taken as shown in Fig. 8. As mentioned earlier, the angle of repose under cylindrical conditions varies with the direction of measurement due to the discrepancy between the cylinder centre and the apex of the sand heap. The angle of repose θ_i was determined for

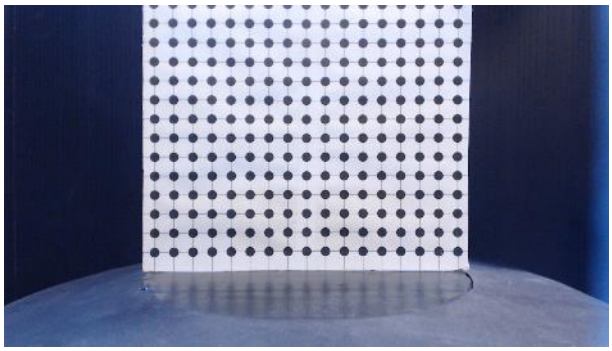

Figure. 4 Geometric correction marks

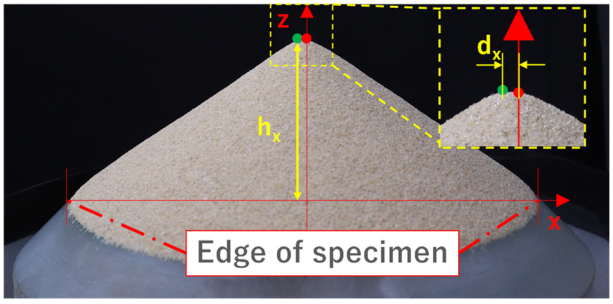

Figure. 5 A schematic diagram of the quantities to be measured on the verification specimen

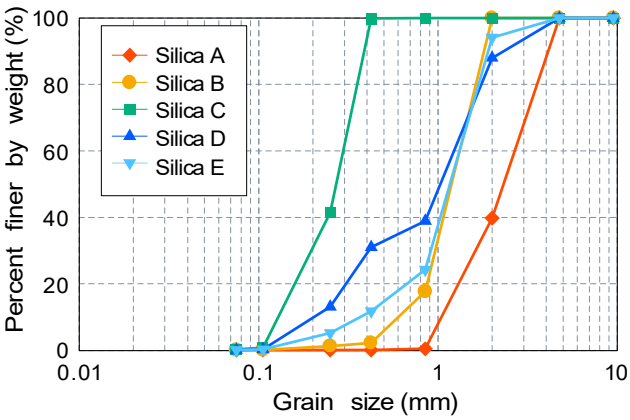

Figure. 6 Grain size distribution

each line connecting point i with the apex of the sand heap. 360 measuring points i were set up at equal intervals at the top of the cylindrical wall. Next, draw a perpendicular line from the apex to the bottom of the sand heap. Draw an X-X' line passing through the point where that perpendicular line intersects the bottom of the sand heap and an arbitrary measurement point i divided by 360.

Table 2. List of materials properties

Sample name	Material	Ratio of Materials (Silica No.3A: Silica No.4: Silica No.6)	D_{60} (mm)	D_{50} (mm)	D_{10} (mm)	U_c	U_c'
Silica A	Silica No.3A	1:0:0	2.92	2.47	1.13	2.59	0.89
Silica B	SilicaNo.4	0:1:0	1.44	1.30	0.64	2.27	1.14
Silica C	Silica No.6	0:0:1	0.31	0.28	0.14	2.21	1.04
Silica D	Mix Silica 1	1:1:1	1.43	1.15	0.21	6.98	0.51
Silica E	Mix Silica 2	1:8:1	1.44	1.27	0.38	3.83	1.65

The angle between the X-X' line and the line passing through the apex of sand heap and measurement point i was calculated as θ_i. When this X-X' line is drawn, two points of intersection are created on the circumference of the top of the cylindrical wall, including measurement point i. Of the side divided by the two points on the circumference and the point where the perpendicular line from the apex intersects the X-X' line, L_{max} is the long side and L_{min} is the short side. Geometrically, the angle between L_{max} and the straight line connecting the point on the circumference and the top of the sand heap is the minimum angle of repose θ_{min}, and the angle between L_{min} and the straight line is the maximum angle of repose θ_{max}. In this study, the first angle of repose, which takes into account the position of the vertex in three dimensions, is defined as the mean angle of repose θ_i^{ave}, which is the average value of i, and the second angle of repose is defined as the maximum-minimum mean angle of repose θ_{mm}^{ave}, which is given as the average of the maximum and minimum angles of repose. Note that since θ_i divides the circumference into 360 equal parts, the points on the circumference that represent the maximum and minimum angles of θ_i do not necessarily coincide with the points that are L_{max} or L_{min}.

$$\theta_i^{ave} = \frac{\sum_1^{360} \theta_i}{360} \quad (1)$$

$$\theta_{mm}^{ave} = \frac{\theta_{max} + \theta_{min}}{2} \quad (2)$$

As a third method, the angle is calculated from the height of the sand heap and the radius of the cylinder using Eq. (3) below, without considering the horizontal position of the apex, which has been used in previous studies and is defined as the simple angle of repose.

$$\theta = atan\left(\frac{h}{r_B}\right) \quad (3)$$

Where h is the height of the sand heap for each experiment n and r_B is the radius of the cylinder, 80 mm. Finally, the angles were determined by a two-dimensional method from the images obtained. The method is based on the angle between the straight line passing through the apex of the sand heap and the horizontal line passing through the points l, m, n and o, which the left or right edge of the sand heap on the two pictures is defined as θ_l, θ_m, θ_n and θ_o, respectively. These angles were then averaged and defined as the plane angle of repose θ_{2D}, as shown in Eq. (4).

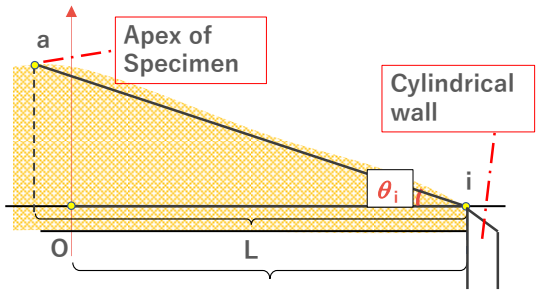

Figure. 8 Definition of angle of repose

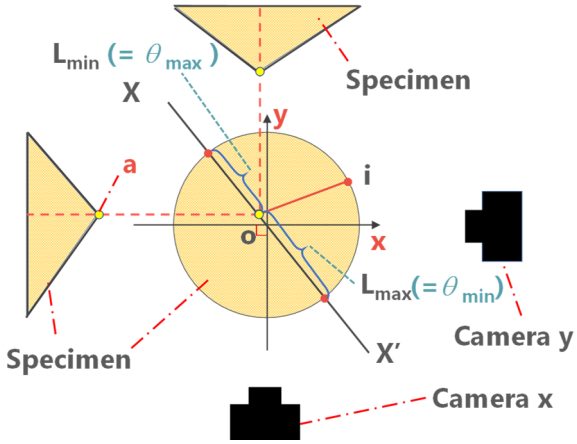

Figure. 7 Schematic diagram for identification of apex by two images and for setting of angle of repose, θ_i

$$\theta_{2D} = \frac{\theta_l + \theta_m + \theta_n + \theta_o}{4} \quad (4)$$

Experiments were conducted twice for each sample. Table 3 lists the initial dry density of the sand for each Table 2 List of materials properties experiment before it was fluidized and the four angles of repose at 90 mm of cylindrical wall displacement. Although there are some slight differences in the initial density, no correlation was found between the angle of repose and the initial dry density at any of the angles of repose within the range of differences in the initial dry densities of the experiments conducted here. Comparisons of the respective angles of repose show generally similar values. These results can be attributed to the fact that the apex of the sand heap was generally located at the centre of the cylinder in the experimental results for the sand used in this study. This indicates shows that a simple method can be used to obtain a highly accurate angle of repose in the case of

Table 3. List of results for dry density and defined angle of repose

Sample name	Dry density(g/cm^3)	θ_i^{ave} (deg.)	θ_{mm}^{ave}	θ	θ_{2D}
Silica A	1.233	40.90	40.93	40.90	40.86
Silica B	1.241	38.51	38.52	38.51	38.45
Silica C	1.304	37.27	37.28	37.27	37.22
Silica D	1.460	41.02	41.02	41.04	40.96
Silica E	1.317	40.32	40.32	40.32	40.26

samples where the apex of the sand heap is at the centre of the cylinder.

As these results are close value, the results for the maximum minimum angle of repose θ_{mm}^{ave} are presented below as representative.

Fig. 9 shows an example of the relationship between the maximum minimum angle of repose and the amount of cylindrical wall movement for each specimen. The reason why the initial value for each specimen is not zero is that the camera is positioned slightly higher than the space of specimen (a) to ensure the highest accuracy around the height of the apex of the final sand heap, as shown in Fig.3. The magnified results at the point of 80-90 mm of side wall movement of Silica C are also shown in Fig. 10.

As can be seen from Fig. 10, the increase in angle of repose for all the specimens decreases after the cylindrical wall movement exceeds approximately 60 mm, followed by an increase and decrease slightly. While no distinction is made in geotechnical engineering, in powder engineering the angle of repose is considered to be the angle of the sand heap at which the angle of the sand heap reaches its limit and the particles start to slide "angle of movement" and the angle at which the particles finish sliding "angle of repose". The slight periodic increase and decrease shown in Fig. 10 is assumed to be the result of the "relaxation angle", which is the difference between the "angle of movement" and the "angle of repose", as the cylindrical wall descends beyond a certain height and repeats this limiting state and the state of repose.

It can be inferred from this result that the angle of repose measured in a stationary state indicates the inclination angle of the sand heap at a certain point in time. By continuously acquiring and averaging the inclination angle of a sand heap in a steady state using this device, the mean and sample standard deviation of the "angle of repose in geotechnical engineering" can be obtained in a single experiment, suggesting the possibility of obtaining a highly accurate angle of repose in a few experiments. Note that all the samples in this experiment were mainly composed of silica, so more types of samples are needed to confirm the results. Table 4 shows the mean and sample standard deviation of the maximum minimum angle of repose $\theta_{mm}^{ave(80\text{-}90)}$ at a cylindrical wall movement of 80-90 mm, respectively.

Fig. 11 shows the relationship between the maximum minimum angle of repose $\theta_{mm}^{ave(80\text{-}90)}$ and the particle size ratio D_B/D_{50} between the specimen base width D_B and the

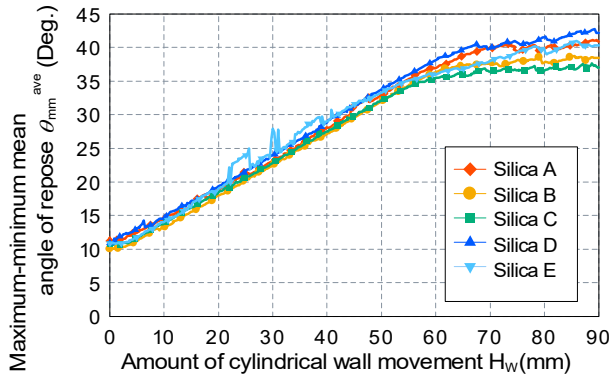

Figure. 9 Relationship between the maximum minimum angle of repose and the amount of cylindrical wall movement

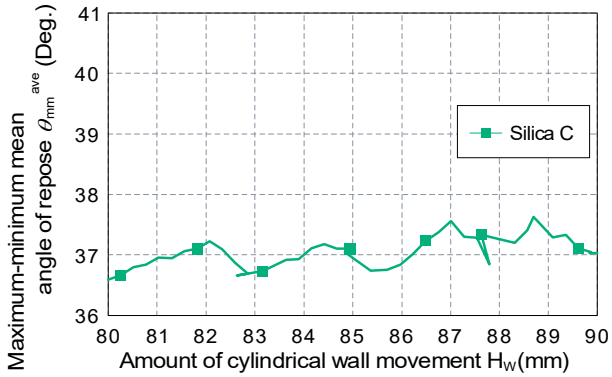

Fig. 10 Relationship between the maximum minimum angle of repose and the amount of cylindrical wall movement for Sample C

mean grain size D_{50}. Fig. 11 also shows the angle of repose with the same definition as simple angle of repose measured by Miura et al. (1997) using Toyoura sand in a cylindrical container. Although the roughness of the bottom of the specimen is different due to the different measuring equipment, the comparison is made as it is because the effect of the roughness of the specimen bottom on the angle of repose is small according to Miura et al(1997). The results of Miura et al. (1997) show that the angle of repose tends to decrease with the power function of the width D_B of the bottom of the specimen. While the maximum minimum angle of repose $\theta_{mm}^{ave(80\text{-}90)}$ tends to decrease with the power function of the bottom width ratio, Silica D and E have larger values than Silica B, which has a similar particle size ratio.

Table 4. Number of samples of the mean and standard deviation of the angle of repose measured between 80-90 mm of sidewall movement $\theta_{mm}^{ave(80\text{-}90)}$

Sample name	Angle of repose $q_{mm}^{ave(80\text{-}90)}$ (Deg.)	Sample standard deviation (Deg.)
Silica A	40.61	0.42
Silica B	38.37	0.29
Silica C	37.16	0.26
Silica D	41.08	0.89
Silica E	40.16	0.53

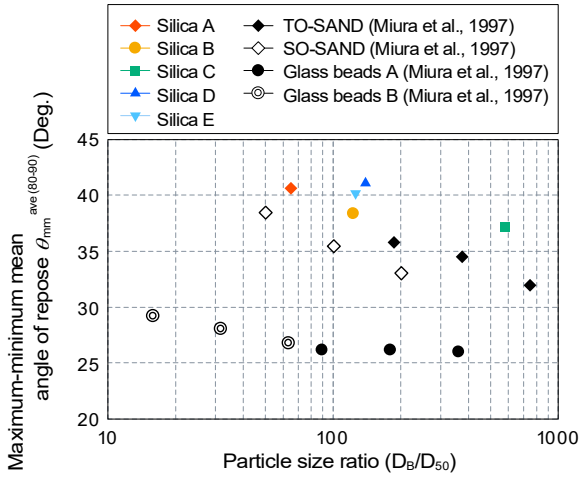

Figure. 12 Relationship between the maximum minimum angle of repose $\theta_{mm}^{ave(80\text{-}90)}$ and the particle size ratio D_B/D_{50}

Fig. 12 shows the relationship between the maximum minimum angle of repose $\theta_{mm}^{ave(80\text{-}90)}$, the mean grain size D_{50} and the 20% grain size D_{20}. In Silica A-C, which is adjusted by the manufacturer for particle size and has a similar particle size distribution, the angle of repose tended to increase linearly with increasing particle size for both the 20% grain size D_{20} and the mean grain size D_{50}. On the other hand, for mixed samples, especially Silica D with a stepped grain size distribution, the angle of repose was found to be higher than Silica A - C at the same 20% grain size D_{20} and mean grain size D_{50}.

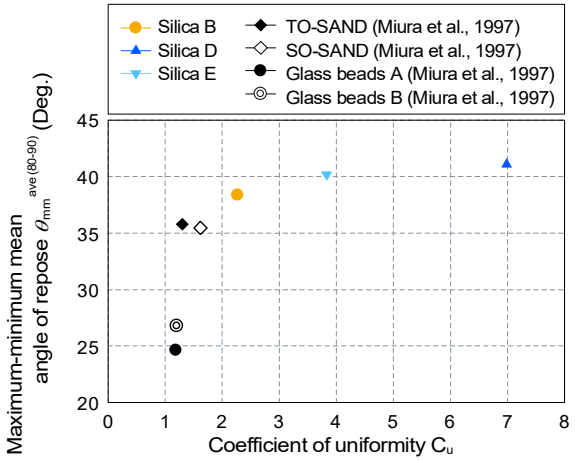

Figure. 13 Relationship between the maximum minimum angle of repose $\theta_{mm}^{ave(80\text{-}90)}$, the mean grain size D_{50} and the 20% grain size D_{20}

Fig. 13 shows the relationship between the maximum minimum angle of repose $\theta_{mm}^{ave(80\text{-}90)}$ and coefficient of uniformity for a particle size ratio D_B/D_{50} of about 100. The figure also shows the results of Miura et al. (1997) for each sample with a particle size ratio close to 100. From the figure, it is clear that the angle of repose increases logarithmically as the coefficient of uniformity increases. However, it should be noted that the glass beads are spherical and therefore peculiarities of the particle shape should be taken into account. A high correlation has been reported between the internal friction angle and the coefficient of uniformity (Rasti et al., 2021), with the internal friction angle increasing logarithmically with respect to the coefficient of uniformity. Given that the angle of repose is a shear phenomenon, these results are considered reasonable. According to Rasti et al. (2021), the relationship between the angle of shear resistance and mean grain size from direct shear tests increases logarithmically. As shown in Fig. 12, this relationship is not logarithmic for the angle of repose but based on the relationship between the internal friction angle and mean grain size, it can be inferred that the angle of repose increases as the mean grain size increases. It is clear that the higher the coefficient of uniformity, the greater the influence of particle size, not the coefficient of uniformity, on the angle of repose.

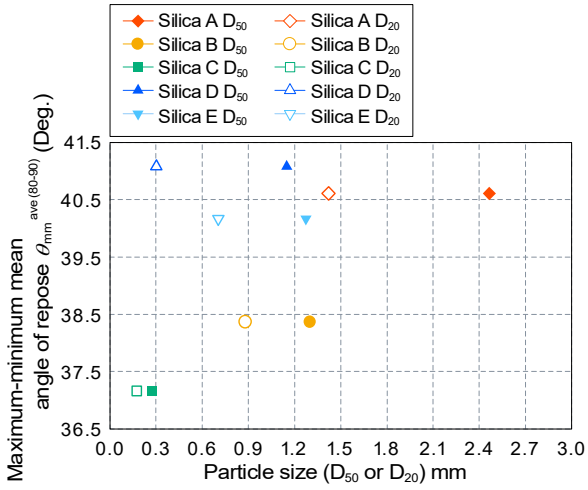

Figure. 11 Relationship between the maximum minimum angle of repose $\theta_{mm}^{ave(80\text{-}90)}$ and coefficient of uniformity

4. Conclusions

In this study, the authors developed a new sidewall velocity-controlled cylindrical angle of repose measurement apparatus that can capture images of a sand heap continuously using two orthogonal cameras in order to reduce the cost of photography. The developed apparatus was used to measure the angle from formation to repose of sand heap using different grain sizes distribution and to assess the effect of grain size distribution on the angle of repose. The findings are summarised as follows.

1. The formation process of the sand heap was continuously measured using the experimental apparatus, and it was found that the sand heap became steady state when it reached a certain height. The angle of repose at which the sand heap became steady state increased and decreased slightly, which is presumed to be the relaxation angle.
2. From conclusion 1, it is inferred that the angle of repose measured in a stationary state indicates the inclination angle of the sand heap at a certain point in time, suggesting the possibility of obtaining a highly accurate angle of repose with fewer experiments by using this experimental apparatus to continuously acquire and average the inclination angle of a sand heap in a steady state.
3. While the maximum minimum angle of repose $\theta_{mm}^{ave(80\text{-}90)}$, as previous studies, tends to decrease with the power function of the bottom width ratio.
4. In the case of sand where the particle size is adjusted by the manufacturer and has a similar particle size distribution, the angle of repose tended to increase linearly with increasing particle size for both the 20% grain size D_{20} and the mean grain size D_{50}. On the other hand, for mixed samples, especially sand with a stepped grain size distribution, the angle of repose was found to be higher than the sand adjusted by the manufacturer at the same 20% grain size D_{20} and mean grain size D_{50}.
5. It was found that the angle of repose increased logarithmically with increasing coefficient of uniformity. Based on these results and conclusions 4, it is clear that the higher the coefficient of uniformity, the greater the influence of particle size, not the coefficient of uniformity, on the angle of repose.

References

Aoki, R. “The measurement of the angle of re-pose and the angle of internal friction of powder and granular materials“, J Research Association of Powder Technology, Japan, 6 (1), pp.3-8, 1969. (in [Japanese]) https://doi.org/10.4164/sptj1964.6.3

ASTM International “Standard Test Method for Meas-uring the Angle of Repose of Free-Flowing Mold Powders (Withdrawn 2005)“, August 16 2017, retrieved October 27, 2022, http://www.astm.org/cgi-bin/resolver.cgi?C1444-00

Botz, J. T., Loudon, C., Barger, J. B., Olafsen, J. S., Steeples, D. W. “Effects of slope and particle size on ant locomotion: Implications for choice of substrate by antlions“, J Kansas Entomological Society, 76 (3), pp.426-435, 2003. https://www.jstor.org/stable/25086130, accessed: 31st/ October/ 2022.

Chen, H., Liu, Y.L., Zhao, X.Q., Xiao, Y.G., Liu, Y. “Numerical investigation on angle of re-pose and force network from granular pile in variable gravitational environments“, Powder Technology, 283, pp.607-617, 2015. https://doi.org/10.1016/j.powtec.2015.05.017

Chik, Z., Vallejo, L. E. “Characterization of the angle of repose of binary granular materials“, Canadian Geotechnical Journal, 42 (2), pp.683-692, 2005. https://doi.org/10.1139/t04-118

Coetzee, C.J., Els, D.N.J. “Calibration of discrete element parameters and the modelling of silo discharge and bucket filling“, Computers and Electronics in Agriculture, 65 (2), 198-212, 2009. https://doi.org/10.1016/j.compag.2008.10.002

Jacques, D. translated by S. Nakanishi and T. Okumura, “Sables, poudres et grains, introduction á la physique des milieux granulaires“, 1st ed., Yoshioka Shoten, Kyoto city, Japan, 2002. (in Japanese)

JIS "R 9301-2-2: Alumina powder – Part2 : Determination of physical properties-2 : Angle of repose“, 1999, https://www.jisc.go.jp/app/jis/general/GnrJISUseWordSearchList?toGnrJISStandardDetailList

Indraratna, B., Sun, Y., & Nimbalkar, S. “Laboratory assessment of the role of particle size distribution on the deformation and degradation of ballast under cyclic loading“, J geotechnical and geoenvironmental engineering, 142(7), 04016016, 2016. https://doi.org/10.1061/(ASCE)GT.1943-5606.0001463

Miura, K., Maeda, K., Toki, S. “Method of measurement for the angle of repose of sands“, Soils and Foundations, 37 (2), pp.89-96, 1997. https://doi.org/10.3208/sandf.37.2_89

Rasti, A., Adarmanabadi, H., Pineda, M., & Reinikainen, J. “Evaluating the effect of soil particle characterization on internal friction angle“, American Journal of Engineering and Applied Sciences, 2021. https://doi.org/10.3844/ajeassp.2021.129.138

Viggiani, G., Küntz, M., & Desrues, J. “An experimental investigation of the relationships between grain size distribution and shear banding in sand“, In Continuous and discontinuous modelling of cohesive-frictional materials, pp.111-127, Springer, Berlin, Heidelberg, 2001. https://doi.org/10.1007/3-540-44424-6_8

Wang, J. J., Zhang, H. P., Tang, S. C., & Liang, Y. “Effects of particle size distribution on shear strength of accumulation soil“, J Geotechnical and Geoenvironmental Engineering, 139(11), pp.1994-1997, 2013. c10.1061/(ASCE)GT.1943-5606.0000931

Wójcik, A., Klapa, P., Mitka, B., & Sładek, J. “The use of the photogrammetric method for measurement of the repose angle of granular materials“, Measurement, 115, pp.19-26, 2018. https://doi.org/10.1016/j.measurement.2017.10.005